Evidence for Synergy between Family 2b Carbohydrate Binding Modules in *Cellulomonas fimi* Xylanase 11A

David N. Bolam,[‡] Hefang Xie,[‡] Peter White,[§] Peter J. Simpson,[¶] Susan M. Hancock,[¶] Michael P. Williamson,[¶] and Harry J. Gilbert*,[‡]

Department of Biological and Nutritional Sciences, University of Newcastle upon Tyne, Newcastle upon Tyne NE1 7RU, U.K., Laboratory of Molecular Enzymology, The Babraham Institute, Babraham, Cambridge CB2 4AT, U.K., and Department of Molecular Biology and Biotechnology, Krebs Institute, University of Sheffield, Sheffield S10 2TN, U.K.

Received November 7, 2000; Revised Manuscript Received December 26, 2000

ABSTRACT: Glycoside hydrolases often contain multiple copies of noncatalytic carbohydrate binding modules (CBMs) from the same or different families. Currently, the functional importance of this complex molecular architecture is unclear. To investigate the role of multiple CBMs in plant cell wall hydrolases, we have determined the polysaccharide binding properties of wild type and various derivatives of *Cellulomonas fimi* xylanase 11A (Cf Xyn11A). This protein, which binds to both cellulose and xylan, contains two family 2b CBMs that exhibit 70% sequence identity, one internal (CBM2b-1), which has previously been shown to bind specifically to xylan and the other at the C-terminus (CBM2b-2). Biochemical characterization of CBM2b-2 showed that the module bound to insoluble and soluble oat spelt xylan and xylohexaose with K_a values of 5.6×10^4, 1.2×10^4, and 4.8×10^3 M^{-1}, respectively, but exhibited extremely weak affinity for cellohexaose ($<10^2$ M^{-1}), and its interaction with insoluble cellulose was too weak to quantify. The CBM did not interact with soluble forms of other plant cell wall polysaccharides. The three-dimensional structure of CBM2b-2 was determined by NMR spectroscopy. The module has a twisted "β-sandwich" architecture, and the two surface exposed tryptophans, Trp 570 and Trp 602, which are in a perpendicular orientation with each other, were shown to be essential for ligand binding. In addition, changing Arg 573 to glycine altered the polysaccharide binding specificity of the module from xylan to cellulose. These data demonstrate that the biochemical properties and tertiary structure of CBM2b-2 and CBM2b-1 are extremely similar. When CBM2b-1 and CBM2b-2 were incorporated into a single polypeptide chain, either in the full-length enzyme or an artificial construct comprising both CBM2bs covalently joined via a flexible linker, there was an approximate 18−20-fold increase in the affinity of the protein for soluble and insoluble xylan, as compared to the individual modules, and a measurable interaction with insoluble acid-swollen cellulose, although the K_a ($\sim 6.0 \times 10^4$ M^{-1}) was still much lower than for insoluble xylan ($K_a = \sim 1.0 \times 10^6$ M^{-1}). These data demonstrate that the two family 2b CBMs of Cf Xyn11A act in synergy to bind acid swollen cellulose and xylan. We propose that the increased affinity of glycoside hydrolases for polysaccharides, through the synergistic interactions of CBMs, provides an explanation for the duplication of CBMs from the same family in some prokaryotic cellulases and xylanases.

The plant cell wall is a highly complex structure comprising primarily the polysaccharides pectin, hemicellulose, and cellulose. Plant cell wall degrading microorganisms express a repertoire of glycoside hydrolases, esterases, and polysaccharide lyases that act in synergy to elicit the degradation of this recalcitrant substrate. These enzymes, particularly those that hydrolyze cellulose and the hemicellulose xylan, have a complex molecular architecture comprising discrete modules, which are normally joined by relatively unstructured linker sequences (*1*). Plant cell wall hydrolases from aerobic microbes typically comprise a catalytic module and one or more carbohydrate binding modules (CBMs)[1] that bind to a polysaccharide within the plant cell wall. CBMs attach the enzyme to the plant cell wall and, by bringing the biocatalyst into intimate and prolonged association with its recalcitrant substrate, increase the rate of catalysis (*2*−*6*). Some CBMs have also been proposed to display additional functions, such as substrate disruption and sequestering and feeding of single cellulose chains into the active site of the catalytic module (*7*−*12*). On the basis of primary structure similarities, CBMs have been grouped into 23 different families, many of which are further divided into subfamilies (*13*). Recently, the tertiary structures of several CBMs from different families have been determined by either nuclear magnetic resonance (NMR) spectroscopy or X-ray crystal-

* To whom correspondence should be addressed. Fax: 0191-2228684; Telephone: 0191-2226962; E-mail: H.J.Gilbert@ncl.ac.uk.
[‡] University of Newcastle upon Tyne.
[§] Laboratory of Molecular Enzymology.
[¶] University of Sheffield.

[1] Abbreviations: AGE, affinity gel electrophoresis; ASC, acid swollen cellulose; BMCC, bacterial microcrystalline cellulose; CBM, carbohydrate binding module; GST, glutathione *S*-transferase; IPTG, isopropyl β-thiogalactopyranoside; ITC, isothermal titration calorimetry.

10.1021/bi002564l CCC: $20.00
Published on Web 02/02/2001

lography. These studies have shown that although the overall fold of most CBMs is conserved, consisting of sandwiched β-sheets, the topology of the actual ligand binding site varies somewhat between the different families. Thus, in families 1, 2a, 3a, 5, and 10, which interact preferentially with crystalline cellulose, the binding site is a flat surface that contains a planar strip of highly conserved aromatic residues that are thought to stack face-to-face against the glucose rings of the polysaccharide (*14*−*18*). The flat surface presumably enables the proteins to interact with the multiple planar chains found in crystalline cellulose. In contrast, in families 4 and 22, the binding site is a shallow cleft that can only interact with a single cellulose or xylan chain, respectively, probably via a combination of stacking interactions and hydrogen bonding (*5*, *19*). Recently, the structure of a family 2b xylan binding module was solved by NMR (*20*). The overall structure of the protein is very similar to that of the cellulose-binding family 2a modules, the main difference being that the surface tryptophans of the family 2b module are arranged in a perpendicular, rather than planar, orientation with respect to one another. This enables the CBM2b to interact with the 3-fold helix of a xylan chain, rather than the planar chains found in cellulose.

Aerobic bacterial cellulases and xylanases often have very complex molecular architectures consisting of multiple CBMs, and sometimes several catalytic modules, in addition to modules of unknown function (*13*). The CBMs in a single enzyme can be members of the same or different protein families (*1*). The evolutionary rationale that led to these complex molecular architectures is currently unclear. It could be argued that multiple CBMs act in synergy to bind to their target ligand, leading to an increased affinity of the enzyme for the polysaccharide. This view is supported by the studies of Linder et al. (*21*) who showed that an artificial protein construct, consisting of two covalently linked family 1 CBMs, had 6−10-fold higher affinity for insoluble cellulose, as compared to the individual modules. Cooperativity between multiple binding sites has also been observed within a single protein module. A recent study has shown that any two of the three discrete ligand binding sites in a protein module from the ricin-like family of CBMs (CBM13) act in synergy to bind xylan (*22*). In contrast, no apparent synergy was observed between the family 2a and family 10 CBMs in *Pseudomonas cellulosa* xylanase 10A (Pc Xyn10A) when the enzyme bound to cellulose (*4*). Similarly, the binding of the duplicated family 4 CBMs in *Cellulomonas fimi* cellulase 9B (Cf Cel9B) to cellulose was found to be independent rather than cooperative (*9*, *23*). Another possible role for the multiple CBMs in plant cell wall hydrolases is that they increase the diversity of polysaccharides that the parent enzyme can interact with (*4*). However, recent studies with the duplicated family 4 CBMs from both *Rhodothermus marinus* Xyn10A and Cf Cel9B have shown that the multiple CBMs in these enzymes share identical ligand specificities (*23*, *24*).

To explore further the suggested roles for multiple CBMs in plant cell wall degrading enzymes, we have dissected the biochemical properties of the different modules of the xylanase, Xyn11A from *C. fimi*, both as single entities and within the complete enzyme. Xyn11A comprises an N-terminal signal peptide that is followed by a glycoside hydrolase family 11 (GH11) catalytic module that exhibits xylanase activity, an internal family 2b CBM (CBM2b-1), a *Rhizobium* NodB homologue (carbohydrate esterase family 4) that displays xylan esterase activity (*25*), and a C-terminal CBM2b (CBM2b-2) that has 70% sequence identity with CBM2b-1. The modules are separated by either proline/threonine- or glycine-rich linkers of approximately 13 residues in length (Figure 1). The full-length xylanase binds to both insoluble xylan and cellulose, while a truncated form of the enzyme, lacking the C-terminal CBM2b, interacted with insoluble xylan but not, apparently, cellulose (*26*−*28*). The internal CBM2b module was previously shown to interact with xylan, but it did not exhibit any significant affinity for cellulose (*20*, *28*, *29*).

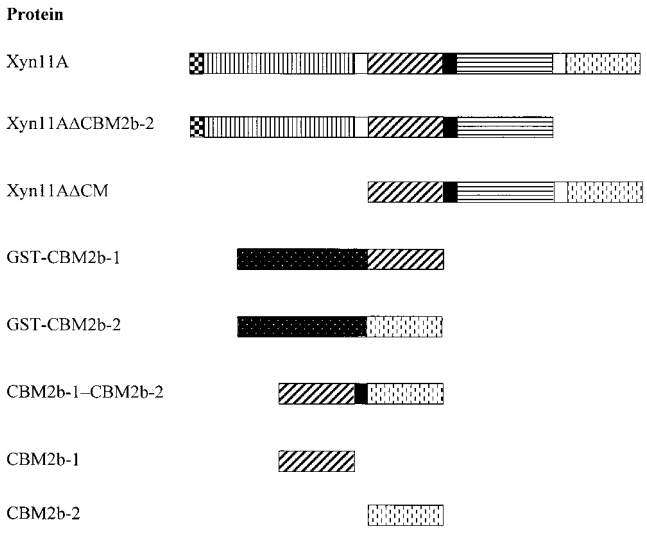

FIGURE 1: Molecular architecture of Cf Xyn11A and its derivatives used in this study. The modules in Xyn11A are as follows: N-terminal signal peptide (cheques), GH11 catalytic module (vertical stripes), glycine linker (white), CBM2b-1 (diagonal stripes), proline/threonine linker (black), NodB homologue (horizontal stripes), CBM2b-2 (vertical dashes). GST is shown as white dots on a black background.

From the discussion above, it is possible that the cellulose binding capacity of Xyn11A is mediated by CBM2b-2, while the enzyme interacts with xylan via CBM2b-1. Alternatively, the association of the xylanase with cellulose could be mediated by synergistic interactions between the two CBM2bs and/or the NodB homologue. To resolve these issues, we have investigated the functional importance of the C-terminal CBM2b in the capacity of the enzyme to bind cellulose and xylan, and determined the 3D-structure of the protein module. The data showed that the biochemical properties and tertiary structures of the C-terminal and internal CBM2b modules of Cf Xyn11A were very similar and, when combined into a single polypeptide chain, they acted in synergy to bind both xylan and cellulose. These results provide an explanation for the presence of multiple CBM2b modules in Cf Xyn11A.

MATERIALS AND METHODS

Sources of Carbohydrates. Wheat arabinoxylan (medium viscosity; Ara:Xyl = 41:59), rye arabinoxylan (Ara:Xyl = 49:51), carob galactomannan (high viscosity; Gal:Man = 21:79), xyloglucan (Tamarind, high viscosity; Ara:Gal:Xyl:Glc = 3:16:36:45), konjac glucomannan (high viscosity; Glu:Man = 40:60, acetylated), β-glucan (barley; high viscos-

ity), debranched arabinan (1,5-α-arabinan; Ara:Gal:Rha:GalUA = 88:4:2:6), pectic galactan (potato; Gal:Ara:Rha:GalUA = 78:9:4:9), rhamnogalacturonan (from soybean pectin), and xylohexaose were from Megazyme International Ireland Ltd. Carboxymethyl cellulose (medium viscosity), 4-*O*-methylglucuronoxylan, and oat spelt xylan (Ara:Xyl = 10:90) were from Sigma. Hydroxyethyl cellulose was from Aldrich. Cellohexaose was from Seikagaku. Bacterial microcrystalline cellulose (BMCC) and acid swollen cellulose (ASC) were prepared essentially as described by Gilkes et al. (*30*) and Abou-Hachem et al. (*24*), respectively. Soluble and insoluble fractions of oat spelt xylan were prepared as described previously (*31*).

Construction of Plasmids. Construction of the plasmid pCF9, which contains full-length Cf *xyn*11A, was described previously (*27*).

To produce the His_{10} tagged version of CBM2b-2, the region of pCF9 that encodes this module was amplified by PCR using the following primers: 5′-CATATGTCGTGCTCGGTGAGCGCC-3′ and 5′-GGATCC**TCA**GCCCGTGGCGCACGTAGC-3′, which contain *Nde*I and *Bam*HI restriction sites, respectively, at their 5′ ends. The three bases highlighted in bold type encode a stop codon. The reactions were performed using $Vent_R$ DNA polymerase (New England BioLabs) according to the manufacturer's protocol. The amplified DNA was ligated into pCR-Blunt (Invitrogen), excised using *Nde*I and *Bam*HI, and cloned into the expression vector pET16b (Novagen).

A similar protocol was used to produce the glutathione *S*-transferase (GST) fusion of CBM2b-2, except that the following primers were used: 5′-GGATCCTCGTGCTCGGTGAGCGCC-3′ and 5′-GAATTC**TCA**GCCCGTGGCGCACGTAGC-3′, which contain *Bam*HI and *Eco*RI sites at their 5′ ends, respectively. The three bases highlighted in bold type encode a stop codon. The amplified CBM2b-2 DNA was cloned into the expression vector pGEX-2T (Pharmacia).

To construct Xyn11AΔCM, the region of pCF9 that encodes CBM2b-1, NodB, and CBM2b-2 was amplified by PCR using the following primers: 5′-CCGCGGCCGTCAGCACCGGCTGCTCGGTC-3′ and 5′-CAGGTCGGATCCCGTCAGCCCGTGGCGCAC-3′, which contain *Cfr*42I and *Bam*HI sites at their 5′ ends, respectively. The plasmid pCF9 was then digested with *Cfr*42I and *Bam*HI, which cut *xyn*11A just after the end of the region encoding the signal peptide and after the 3′ end of the gene, respectively. The fragment comprising the vector and the signal peptide encoding part of *xyn*11A was then purified from a 1% agarose gel and ligated with the similarly digested PCR product to produce *xyn*11AΔCM.

To construct Xyn11AΔCBM2b-2, the region of *xyn*11A that encodes the C-terminal 166 amino acids of the catalytic module and all of CBM2b-1 and the NodB homologue was amplified from pCF9 by PCR using the following primers: 5′-CCCGGGCTCGGTCTCGATGGACCTC-3′ and 5′-GGATCC**TCA**ACCGGCGGACGACGGTGC-3′, which contain *Sma*I and *Bam*HI site at their 5′ ends, respectively. The nucleotides highlighted in bold type encode a stop codon. The plasmid pCF9 was then digested with *Sma*I and *Bam*HI, which cut *xyn*11A 191 nucleotides after the start of the gene and after the 3′ end of the gene, respectively. The fragment comprising the vector and the first 191 nucleotides of *xyn*11A was then purified from a 1% agarose gel and ligated with similarly digested PCR product to produce *xyn*11AΔCBM2b-2.

The W259A and W291A mutants of full-length Xyn11A were produced using the QuikChange Kit (Stratagene) according to the manufacturer's protocol with the following pairs of primers: 5′-CGCGCCGAGGAGGCCTCGGACCGCTTC-3′ and 5′-GAAGCGGTCCGAGGCCTCCTCGGCGCG-3′ for the W259A mutation; 5′-ACCATCCAGGCGAGCGCTAACGCGAACGTC-3′ and 5′-GACGTTCGCGTTAGCGCTCGCCTGGATGGTC-3′ for the W291A mutation. The plasmid pCF9 was used as the template DNA. Mutants were identified by sequencing using an ABI Prism model 377 automated sequencer.

To construct CBM2b-1-CBM2b-2, the region of *xyn*11A encoding CBM2b-1 and the proline/threonine linker immediately following it were amplified from pCF9 by PCR using the following primers: 5′-CATATGGACACGGGCGGAGGCGGC-3′ and 5′-GGATCCGGGCGTCGGCGTCGGCGTC-3′, which contain *Nde*I and *Bam*HI sites at their 5′ ends, respectively. The amplified DNA was ligated into pCR-Blunt, excised using *Nde*I and *Bam*HI and cloned into pET28a (Novagen) to generate p2b-1PT. The region of *xyn*11A that encodes CBM2b-2 was then amplified from pCF9 using the following primers: 5′-GGATCCTCGTGCTCGGTGAGCGCC-3 and 5′-CTCGAG**TCA**GCCCGTGGCGCACGTAGC, which contain *Bam*HI and *Xho*I sites at their 5′ ends, respectively. The nucleotides highlighted in bold type encode a stop codon. The amplified DNA was ligated into pCR-Blunt, excised using *Bam*HI and *Xho*I and cloned into similarly restricted p2b-1PT to generate CBM2b-1-CBM2b-2.

The W570A and W602A mutants of CBM2b-2 fused to GST were produced using the QuikChange kit (Stratagene) according to the manufacturer's protocol with the following pairs of primers: 5′-CGGGGCGAGGAGGCGGCGGACCGCTTC-3′ and 5′-GAAGCGGTCCGCCGCCTCCTCGCCCCG-3′ for the W570A mutation; and 5′-GTGCAGAGCAGCGGGAACGCGGCGCTG-3′ and 5′-CAGCGCCGCGTTCCCGCTGCTCTGCAC-3′ for the W602A mutation. The plasmid containing CBM2b-2 in pGEX-2T was used as the template DNA.

All DNA constructs were sequenced to ensure no nonspecific mutations had occurred during the cloning procedure.

Production of Recombinant Proteins. Escherichia coli strains used in this study were JM83 (*32*) and BL21 (DE3): pLysS (*33*). Recombinant *E. coli* was cultured in Luria broth (2.4 L) supplemented with 100 μg/mL ampicillin at 30 °C (JM83) or 37 °C (BL21). The cells were grown to mid-log phase before gene expression was induced by the addition of 0.5 mM (JM83) or 1 mM (BL21) IPTG and the bacteria were incubated for a further 3−4 h. *E. coli* JM83 was used to express the GST fusion proteins and pCF9 derivatives, while the His-tagged CBMs were produced in *E. coli* BL21 (DE3):pLysS. In cultures containing pCF9 or derivatives, gene expression was constitutive and so the cells were simply grown for 16 h after inoculation.

Purification of Recombinant Proteins. Full-length Xyn11A, Xyn11AΔCM, Xyn11AΔCBM2b-2, and the W259A and W291A mutants of full-length Xyn11A were purified by cellulose affinity chromatography essentially as described previously (*27*). GST and GST fusion proteins were purified

using Glutathione Sepharose (Pharmacia) affinity chromatography as described previously (*20*). His tagged proteins were purified using immobilized metal affinity chromatography (TALON resin; ClonTech) as described previously (*3*).

Affinity Gel Electrophoresis (AGE). The capacity for the GST fusion of CBM2b-2 to bind to a variety of soluble plant structural polysaccharides was evaluated by affinity electrophoresis. Continuous native polyacrylamide gels were prepared consisting of 7.5% (w/v) acrylamide in 25 mM Tris/250 mM glycine buffer, pH 8.3. To one of the gels, 0.1% polysaccharide was added prior to polymerization. Approximately 5 μg of target proteins and GST (as a noninteracting negative control) were loaded on the gels and subjected to electrophoresis at 10 mA/gel for 2 h at room temperature. Proteins were visualized by staining with Coomassie Blue.

Binding Isotherms. Binding isotherms were performed on ice in 50 mM sodium phosphate buffer, pH 7.0, at protein concentrations ranging from 1 to 100 μM. Protein (250 μL) was added to 0.25 mg of ASC, BMCC, or insoluble oat spelt xylan and incubated for 1 h with gentle mixing. The polysaccharide was centrifuged at 13000*g* for 1 min, and the A_{280} of the supernatant was measured to quantify the amount of free protein remaining after binding. Bound protein was calculated from the total minus the free protein. Binding isotherms were also performed with GST (a control for nonspecific binding). The data were analyzed by nonlinear regression using a standard one-site binding model (GraphPad Prism, v2.01), and the N_0 and K_a values were obtained from the regressed isotherm data. At least three separate binding isotherms were carried out for each protein.

Isothermal Titration Calorimetry (ITC). ITC measurements were made at 25 °C using a MicroCal Omega titration calorimeter. Proteins were dialyzed extensively against 50 mM sodium phosphate buffer, pH 7.0, and the ligand was dissolved in the dialysis buffer. During a titration, the protein sample (60−300 μM), stirred at 400 rpm in a 1.3586 mL reaction cell, was injected with 25 successive 10 μL aliquots of a stock oat spelt xylan solution (6.6 mg/mL) at 200 s intervals. Given that the protein binds to six successive xylose residues (*20*), and the binding cleft comprises the complete length of the CBM, the ligand was deemed to comprise nonoverlapping xylohexaose units within the xylan molecules. The ligand concentration was therefore taken to be the nonoverlapping xylohexaose concentration in the xylan, which equates to 7.4 mM (taking into consideration that oat spelt xylan contains 10% arabinose). This assumption was strongly supported by the ITC data, which showed that the stoichiometry of binding was close to unity when defining the ligand as six consecutive xylose units. Raw binding data were corrected for heat of dilution of both protein and ligand. Integrated heat effects were analyzed by nonlinear regression using a single-site binding model (MicroCal ORIGIN, v2.9), yielding values for the K_a and $\Delta H°$. Other thermodynamic parameters were derived from the equation $-RT \ln K_a = \Delta G° = \Delta H° - T\Delta S°$.

NMR Studies. Samples subjected to NMR were typically 0.7−1.0 mM in 50 mM sodium phosphate buffer, pH 5.0, containing 10 mM sodium azide and 0.1 mM sodium 3-trimethylsilyl-2,2,3,3-d_4-propionate. NMR studies were carried out on Bruker DRX-500 and 600 spectrometers. Titrations for measurement of affinity constants were carried out as described previously (*4*), using the resonances of Trp 570 and Trp 602. Structural studies used unlabeled and ^{15}N-labeled protein. Assignment of ^{1}H and ^{15}N resonances was essentially complete, and a list has been deposited in BioMagResBank (accession number BMR4900). Restraints were obtained from 2D NOESY and 3D ^{15}N-filtered NOESY (mixing times 100 ms), from E.COSY, HNHA, and HNHB spectra, and using exchange of HN and HN chemical shift temperature coefficients to characterize amide groups involved in hydrogen bonds (*20*, *29*, *34*). In initial rounds of calculation, only unambiguous NOEs and φ dihedral restraints were included, together with the single disulfide bond. In subsequent rounds, further NOE restraints, including ambiguous restraints (*35*), were added, along with side chain dihedral restraints, stereoassignments, and hydrogen bonding restraints. Structures were calculated by hybrid distance geometry/simulated annealing in XPLOR, as described previously (*20*, *29*). The ensemble of structures selected had no distance violations greater than 0.50 Å and no dihedral angle violations greater than 5°. The ensemble was superimposed on the lowest energy structure, averaged, and energy minimized to obtain a single representative structure. This structure and representative members of the ensemble have been deposited in the Protein Data Bank (accession codes1hej and 1heh, respectively).

RESULTS

Xyn11A Derivatives Used in This Study. To investigate the importance of the different modules of Cf Xyn11A in polysaccharide binding, various derivatives of the enzyme were generated and purified by affinity chromatography to electrophoretic homogeneity. A schematic of the Cf Xyn11A derivatives used in this study is presented in Figure 1.

The Binding of Full-Length Xyn11A to Insoluble Forms of Cellulose. The interaction of full-length Cf Xyn11A with bacterial microcrystalline cellulose (BMCC) and acid swollen cellulose (ASC) was studied using binding isotherms. The data, presented in Figure 2 and Table 1, indicated that the enzyme had significant affinity for ASC but shows no binding to BMCC above that of the nonspecific control of GST alone.

Ligand Specificity of Xyn11A CBM2bs. In a recent study, we showed that CBM2b-1 bound to soluble oat spelt xylan and xylohexaose but displayed no affinity for soluble forms of other plant cell wall carbohydrates, including soluble forms of cellulose, although a very weak interaction with cellohexaose could be detected by NMR (*20*). In addition, it has previously been shown that full-length Cf Xyn11A bound to cellulose and xylan, but a derivative of the xylanase lacking the C-terminal CBM2b had lost the capacity to bind to cellulose, but not xylan (*28*). It is possible, therefore, that CBM2b-2 and CBM2b-1 mediated cellulose and xylan binding, respectively. To test this hypothesis further, CBM2b-1 and CBM2b-2 were expressed as discrete entities and the binding of these proteins to cellulose and xylan was assessed quantitatively. In addition, GST alone was used as a noninteracting negative control. The binding isotherm data, shown in Figure 3 and Table 1, indicated that both CBM2b-1 and CBM2b-2 bound to insoluble oat spelt xylan with similar affinities. Binding of both CBMs to ASC was slightly higher than the nonspecific control of GST alone, although this

Table 1: Binding of Xyn11A and Derivatives to Insoluble Ligands

protein	insoluble xylan		ASC	
	K_a (M^{-1})	N_0 (μmol/g)	K_a (M^{-1})	N_0 (μmol/g)
full-length Xyn11A	–[a]	–	$6.4 (\pm 0.6) \times 10^4$	9.6 ($\pm$ 1.4)
CBM2b1-CBM2b-2	$1.0 (\pm 0.5) \times 10^6$	28.2 ($\pm$ 5.1)	$5.5 (\pm 1.2) \times 10^4$	9.4 ($\pm$ 0.6)
Xyn11AΔCM	$1.1 (\pm 0.4) \times 10^6$	27.4 ($\pm$ 4.3)	–	–
Xyn11AΔCBM2b-2	–	–	ND[b]	ND
full-length W259A	–	–	ND	ND
full-length W291A	–	–	ND	ND
CBM2b-1	$4.7 (\pm 1.9) \times 10^4$	58.5 ($\pm$ 6.0)	ND	ND
CBM2b-2	$5.6 (\pm 2.2) \times 10^4$	56.6 ($\pm$ 11.7)	ND	ND

[a] Not tested. [b] No significant binding detectable by isotherms.

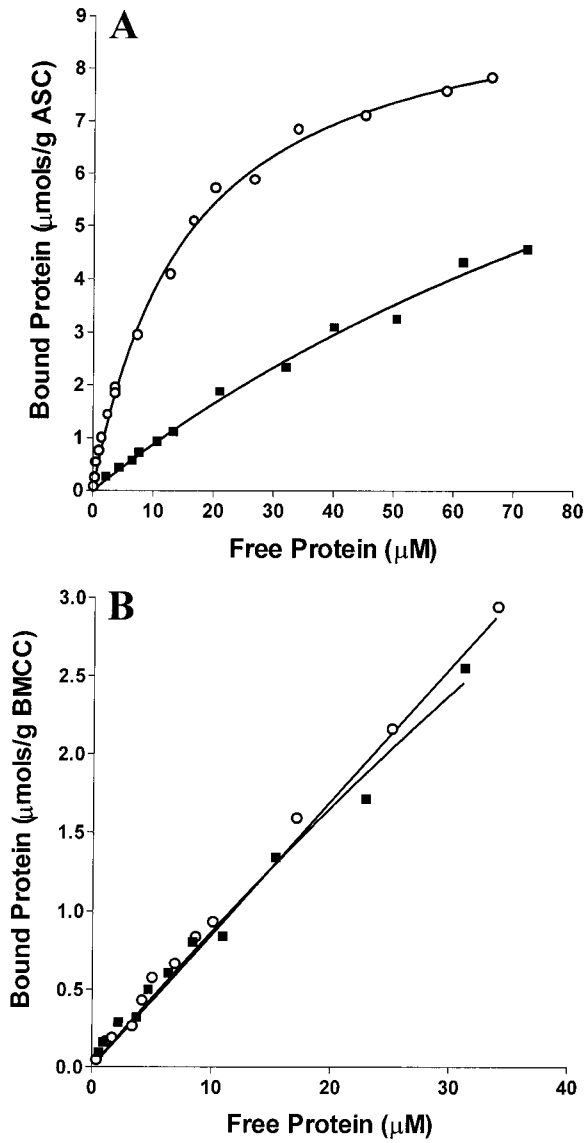

FIGURE 2: Binding isotherms of full-length Xyn11A and GST against ASC (A) and BMCC (B). Adsorption measurements of full-length Xyn11A (○) and GST alone (■) were performed on ice in 50 mM sodium phosphate buffer, pH 7.0, as described in Materials and Methods.

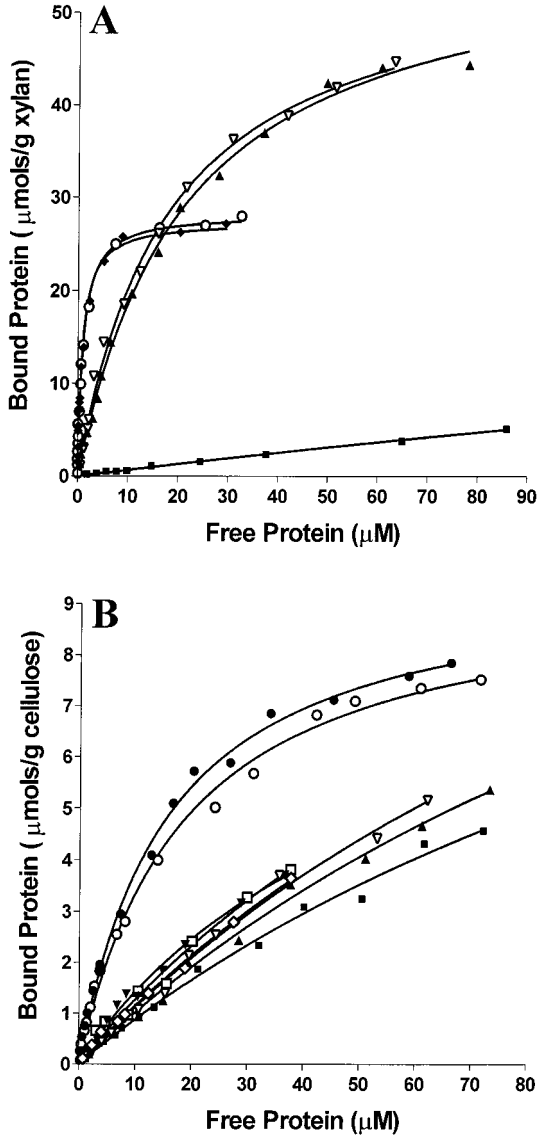

FIGURE 3: Binding isotherms of derivatives of Xyn11A against insoluble oat spelt xylan (A) and ASC (B). Adsorption measurements of full-length Xyn11A (●), Xyn11AΔCM (◆), CBM2b-1-CBM2b-2 (○), CBM2b-1 (▲), CBM2b-2 (▽) W259A in full-length Xyn11A (▼), W291A in full-length Xyn11A (□), Xyn11A-ΔCBM2b-2 (◊) and GST (■) were performed on ice in 50 mM sodium phosphate buffer, pH 7.0, as described in Materials and Methods.

affinity was too low to be quantified as the binding isotherm did not approach saturation. Affinity gel electrophoresis (AGE) was used to evaluate the capacity of the GST fusion of CBM2b-2 to interact with soluble polysaccharides. The results (Figure 4) showed that, in common with CBM2b-1 (*20* and Figure 4), the module bound to both oat spelt xylan (a relatively unsubstituted polysaccharide) and heavily substituted arabinoxylans from wheat and rye, as well as methylglucuronoxylan, and also to barley β-glucan. The module did not associate with soluble forms of cellulose, (carboxymethyl cellulose or hydroxyethyl cellulose), xylo-

Table 2: Binding of Xyn11A Derivatives to Soluble Ligands

protein	ligand	K_a (M^{-1})	$\Delta G°$(kcal mol^{-1})	$\Delta H°$(kcal mol^{-1})	$T\Delta S°$(kcal mol^{-1})	n
CBM2b-1	soluble xylan[a]	$5.9 (\pm 0.2) \times 10^3$	$-5.1 (\pm 0.02)$	$-11.8 (\pm 0.18)$	$-6.7 (\pm 0.2)$	$1.10 (\pm 0.06)$
	xylohexaose[b,c]	3.4×10^3				
	cellohexaose[b,c]	$<1.0 \times 10^2$				
CBM2b-2	soluble xylan[a]	$1.2 (\pm 0.1) \times 10^4$	$-5.6 (\pm 0.01)$	$-13.8 (\pm 0.44)$	$-8.2 (\pm 0.4)$	$1.05 (\pm 0.08)$
	xylohexaose[c]	4.8×10^3				
	cellohexaose[c]	$<1.0 \times 10^2$				
CBM2b-1- CBM2b-2	soluble xylan[a]	$1.6 (\pm 0.1) \times 10^5$	$-7.1 (\pm 0.04)$	$-10.0 (\pm 0.15)$	$-2.9 (\pm 0.2)$	$2.19 (\pm 0.11)$

[a] Data determined by ITC. [b] Data from ref *20* (determined by NMR). [c] Data determined by NMR.

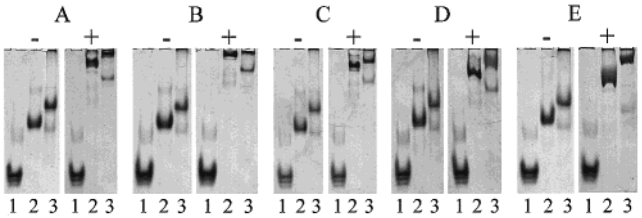

FIGURE 4: Affinity gel electrophoresis of GST fusions of CBM2b-1 and CBM2b-2 against various soluble plant cell wall polysaccharides. GST alone (lane 1), CBM2b-1 (lane 2), and CBM2b-2 (lane 3) were electrophoresed in 7.5% nondenaturing polyacrylamide gels containing no polysaccharide (−) or 0.1% (w/v) rye arabinoxylan (A+), wheat arabinoxylan (B+), oat spelt xylan (C+), methylglucuronoxylan (D+), and barley β-glucan (E+).

glucan, carob galactomannan, konjac glucomannan, debranched arabinan, potato galactan, or rhamnogalacturonan (data not shown). To investigate the capacity of CBM2b-2 to interact with soluble oligosaccharides, the NMR spectra of the protein titrated with xylohexaose and cellohexaose were recorded. The data showed that there was a considerable downfield movement in the chemical shift of the side chain NH^{ϵ} resonances of two solvent-exposed tryptophan residues (Trp 570 and Trp 602) during titration with the xylooligosaccharide. These chemical shift changes were used to calculate the K_a of the protein for xylohexaose, which was estimated to be 4.8×10^3 M^{-1} (Table 2). Titration with cellohexaose also caused a change in the chemical shift of the same two tryptophan signals; however, the estimated K_a was very low ($<1.0 \times 10^2$; Table 2). The resonances affected by titration with xylohexaose correspond very closely with the equivalent residues seen on titration of CBM2b-1 with xylohexaose (*20*). These data indicate that the biochemical properties of CBM2b-2 are very similar to CBM2b-1. Both modules are essentially xylan binding proteins that exhibit a very weak affinity for cellohexaose and ASC. It would appear, therefore, that the capacity of Cf Xyn11A to bind to cellulose is not mediated exclusively by the C-terminal module but rather is a cooperative property of the whole protein.

Synergy between CBM2b-1 and CBM2b-2 in Full-Length Xyn11A Binding to Cellulose and Xylan. In view of the data described above, it is unlikely that the cellulose-binding capacity of Cf Xyn11A is mediated by a single module. It is probable that the binding of the xylanase to cellulose involves the cooperative interaction between two or more modules of the enzyme. To investigate this possibility, various derivatives of the glycoside hydrolase were generated, and their association with insoluble cellulose was evaluated. The data, presented in Figure 3 and Table 1, showed that while the full-length enzyme bound to ASC, removal of either the C-terminal CBM (Xyn11AΔCBM2b-2), or inactivation of CBM2b-1, through mutation of Trp 259 or Trp 291 to alanine in the full-length enzyme, effectively destroyed the capacity of the protein to interact significantly with the cellulose. In contrast, combining CBM2b-1 and CBM2b-2 into a single polypeptide, generated a protein that bound to cellulose with an affinity similar to native Cf Xyn11A. These results indicate that the capacity of Xyn11A to bind to ASC is mediated by the synergistic interaction of the two family 2b CBMs of this enzyme and not by the catalytic module or NodB homologue.

To determine the influence of the different modules of Cf Xyn11A on its interaction with xylan, the capacity of CBM2b-1-CBM2b-2 and a truncated form of Xyn11A lacking the GH11 catalytic module (Xyn11AΔCM) to interact with insoluble xylan was assessed using binding isotherm measurements. Removal of the catalytic module was necessary as enzymatic degradation of the xylan prevented accurate isotherm measurements with the full-length enzyme. The data, presented in Figure 3 and Table 1, showed that the Xyn11AΔCM and CBM2b-1-CBM2b-2 derivatives of the enzyme bound approximately 20 times more tightly to the insoluble hemicellulose than the individual CBM2bs. The results also showed that CBM2b-1-CBM2b-2 bound to xylan with approximately 18-fold higher affinity than with ASC. In addition, the affinity of both individual CBM2bs and CBM2b-1-CBM2b-2 for soluble oat spelt xylan was determined by ITC. The data (Table 2) showed that the linked CBM construct had an affinity for soluble xylan approximately 18 times higher than the individual CBM2bs. The ITC results also showed that, in common with CBM2b-1, the binding of CBM2b-2 and CBM2b-1-CBM2b-2 to xylan is enthalpically driven, with entropy contributing unfavorably to the interaction (Table 2).

Overall, these data indicate that in native Cf Xyn11A, the two CBM2bs act in synergy to bind cellulose and soluble and insoluble xylan.

3D-Structure of CBM2b-2. Given the level of identity between the primary structures of CBM2b-1 and CBM2b-2 (70%) and their similar biochemical properties, one might expect that their 3D-structures will also be very similar. However, it is necessary to characterize the structure of both modules thoroughly, because it is now established that CBMs with similar primary structure can have very different binding properties (*5*, *20*, *29*). The structure of CBM2b-2 was therefore determined using NMR spectroscopy, using standard 2D and 3D methods on ^{15}N-labeled and unlabeled protein. The structure is shown in Figure 5, and structural statistics are compiled in Table 3. On average, one amino acid per structure was found in the disallowed region of the Ramachandran map (*36*). This generally corresponded to a residue found in one of the disordered regions of the NMR

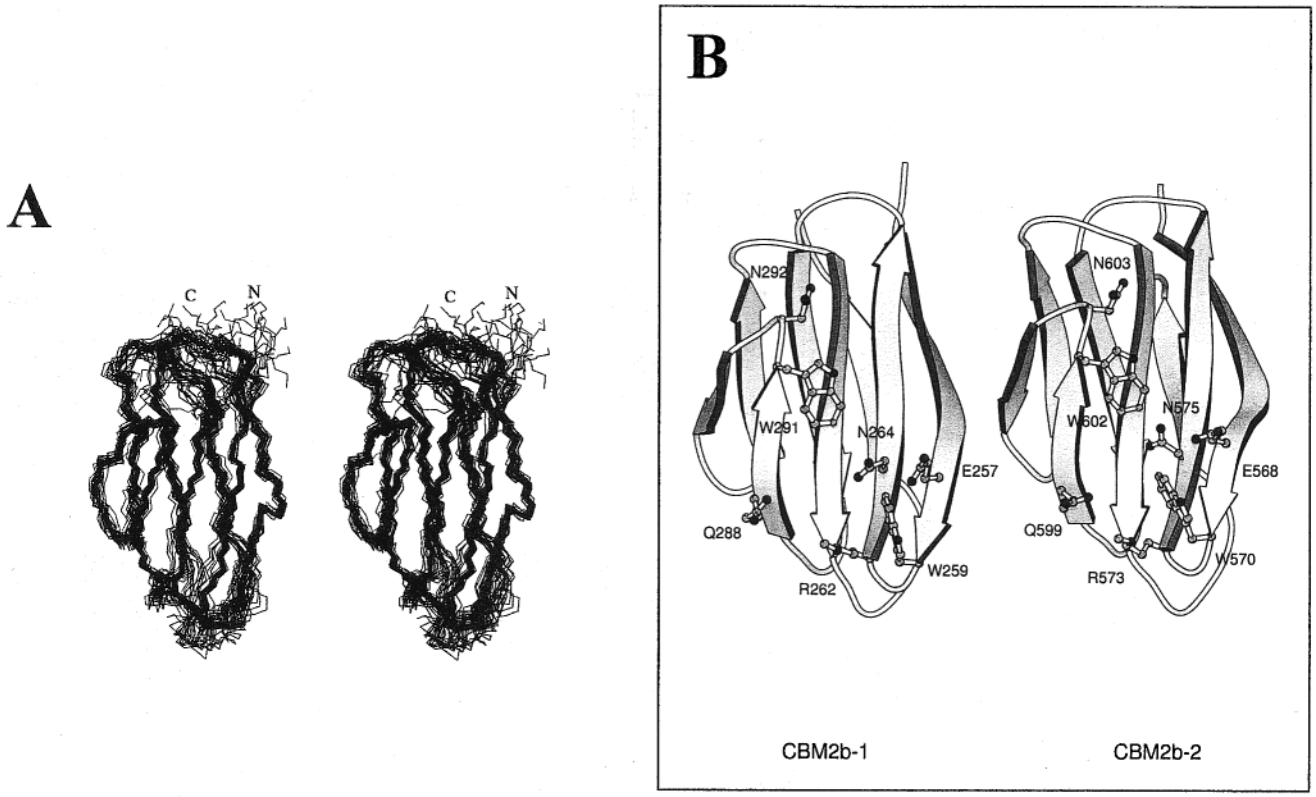

FIGURE 5: Backbone structure of CBM2b-2. (A) Superposition of the 23 structures selected from 50, shown as a stereo diagram. The superposition used the backbone atoms (N, Cα, C′) of residues in regular secondary structure elements (residues 560−570, 573−581, 586−592, 596−602, 604−608, 612−617, 622−630, 637−641) (B) MOLSCRIPT (*42*) representation of CBM2b-1 and CBM2b-2, based on the minimized averaged structures. The conserved residues in the ligand binding site of both CBMs are indicated.

Table 3: Structural Statistics for the Family of 23 Calculated Structures of CBM2b-2 and the Minimized Averaged Structure

	<**CBM2b-2**>[a]	**CBM2b-2**$_{av-min}$[a]
rmsd from experimental restraints		
distance restraints [935] (Å)[b]	0.029 ± 0.002	0.02
dihedral restraints [94] (°)[c]	0.47 ± 0.14	0.46
rmsd from idealized covalent geometry		
bonds (Å)	0.002 ± 0.000	0.002
angles (°)	0.45 ± 0.01	0.43
impropers (°)	0.31 ± 0.01	0.30
X-PLOR energies (kcal mol^{-1})		
E_{total}	129.9 ± 9.4	107.6
E_{NOE}	38.3 ± 6.2	20.8
E_{cdih}	1.4 ± 0.7	1.2
E_{angle}	65.7 ± 2.9	59.3
$E_{improper}$	9.6 ± 0.9	8.6
Ramachandran analysis		
most favored region (%)	67.5	64.8
additionally allowed regions (%)	27.3	31.0
generously allowed regions (%)	3.7	2.8
disallowed regions (%)	1.5	1.4
precision analysis: rmsd to mean structure (Å)		
backbone atoms (secondary structure) (residues 560−640)	0.70 ± 0.13 0.89 ± 0.15	
all heavy atoms (secondary structure) (residues 560−640)	1.08 ± 0.16 1.20 ± 0.16	

[a] <CBM2b-2>: ensemble of 23 structures; CBM2b-2$_{av-min}$: minimized average structure. [b] 52 hydrogen bond restraints, plus 296 intraresidue, 228 sequential, 68 medium-range, 221 long-range, and 70 ambiguous NOEs. [c] 54 ϕ and 40 χ_1 dihedral restraints.

ensemble, particularly Ser 583 and Ser 584, present in the loop connecting strands 2 and 3, and Ser 633 and Ser 634 in the loop linking strands 7 and 8.

The structure of CBM2b-2 is very similar to that of CBM2b-1 (Figure 5; *20*). The secondary structures of the two proteins are essentially identical, with a root-mean-square difference between the backbone atoms of regular secondary structure of only 1.14 Å. All the residues identified previously (*20*, *29*; Xie et al., unpublished data) as being key residues for the interaction of CBM2b-1 with xylan, namely, Glu 257, Trp 259, Arg 262, Asn 264, Gln 288, Trp 291, and Asn 292 (residues 568, 570, 573, 575, 599, 602, and 603, respectively, in CBM2b-2), are conserved in CBM2b-2 and in a similar orientation (Figure 5, panel B). In particular, the two exposed tryptophan residues that control xylan binding are in essentially identical positions, forming the "twisted" binding site topology characteristic of CBM2b-1 (*20*). The closest significant amino acid substitution on the surface of the protein is Met 318 on CBM2b-1, whose corresponding residue in CBM2b-2 is a tyrosine, but these side chains are too far from the binding site for xylan to be involved in any direct interaction.

Role of Trp570, Arg573, and Trp602 in CBM2b-2 Ligand Binding. Recent studies have shown that the two surface tryptophans (Trp 259 and Trp 291) of CBM2b-1 are essential for xylan binding (Xie et al., unpublished data). Furthermore, it was found that the orientation of these two residues relative to one another was pivotal in determining the module's ligand specificity. The tryptophans are perpendicular in the wild-type protein, but on replacing Arg 262 with the smaller glycine residue, the side chain of Trp 259 was caused to rotate approximately 90° so that it lay flat against the protein's surface in a planar orientation with Trp 291. This reorientation of Trp 259 changed the specificity of the mutant

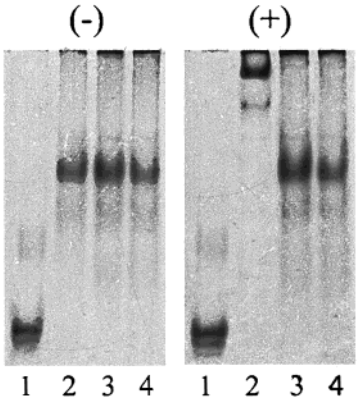

FIGURE 6: Affinity gel electrophoresis of W570A and W602A against vxylan. GST alone (lane 1), wild-type CBM2b-2 fused to GST (lane 2), W570A (lane 3), and W602A (lane 4) were subjected to electrophoresis in 7.5% nondenaturing polyacrylamide gels containing no polysaccharide (−) or 0.1% (w/v) soluble oat spelt xylan (+).

protein such that it bound cellulose but not xylan (*29*). To evaluate whether the surface tryptophans played a similar role in CBM2b-2, the binding properties of the mutants W570A, W602A, and R573G in the isolated module fused to GST were assessed (Arg 573 in CBM2b-2 corresponds to Arg 262 in CBM2b-1; Figure 5, panel B). The data, presented in Figure 6, showed that both tryptophans were essential for xylan binding. In addition, modification of Arg 573, adjacent to Trp 570, altered the specificity of the CBM such that it no longer bound to xylan but interacted with cellulose (data not shown), as observed previously for CBM2b-1 (*29*). These site-directed mutagenesis studies, coupled with the NMR structure of CBM2b-2, support the view that the tertiary structure of this module and the mechanism by which it binds to, and recognizes, its target ligand are essentially identical to those of CBM2b-1.

DISCUSSION

The primary objective of this study was to investigate the biological significance of multiple copies of CBMs in plant cell wall hydrolases. To address this question, we have focused on Xyn11A from *C. fimi*, which contains two copies of a family 2b CBM that exhibits 70% sequence identity with each other. The data presented showed that the two family 2b CBMs bind to soluble and insoluble xylan with approximately 20 times higher affinity when incorporated into a single protein species, than when they were expressed as discrete entities, indicating that, when covalently linked, the modules were acting in synergy to bind the xylose polymer.

Cooperativity between individual sugar binding subsites within a single protein module is well established. For example, the lectin-like family 13 CBMs, which bind to xylan, contain three discrete subsites orientated at 120° to each other. A xylan chain can occupy two of the three sites at any one time. Site-directed mutagenesis studies by Boraston et al. (*22*) showed that these sites acted in synergy to bind the hemicellulose. This is the same phenomenon as that observed in many other lectin/oligosaccharide interactions (*37*, *38*). Similarly, removal of either of the surface tryptophan residues in both Cf Xyn11A CBM2b-1 and CBM2b-2 caused a complete loss of xylan binding to each module, rather than a 2-fold reduction in affinity, indicating that the two aromatic amino acids act cooperatively within each module to bind the polysaccharide (Xie et al., unpublished data). However, in both these examples, synergy occurs between subsites within the same protein module. In contrast, this paper provides the first report of synergy between discrete, but covalently linked, CBMs in a protein that occurs in vivo. The only other demonstration of synergy between discrete covalently linked CBMs was provided by Linder et al. (*21*), who showed that when two family 1 CBMs were joined together in an artificial protein construct, they displayed cooperative binding to cellulose. In the authors' proposed model for the synergism between these modules, binding of one of the CBM1s to an insoluble polysaccharide increases the affinity of the second module for the ligand due to a proximity effect, thus enhancing the overall affinity of the protein construct. The model is also valid for soluble polysaccharides as binding of one module to part of a soluble chain will bring the second linked module into proximity with its ligand. On the basis of the data presented in this paper, we propose that Linder's model for synergy between two flexibly linked CBMs may also apply to Cf Xyn11A and thus can be extended to protein−xylan interactions.

Linder et al. (*21*) also suggest a procedure for quantifying the degree of synergy between the two CBMs. A coupling free energy ΔG^S can be defined, given by

$$\Delta G^S = \Delta G_{12} - (\Delta G_1 + \Delta G_2)$$

where ΔG_{12}, ΔG_1, and ΔG_2 are, respectively, the free energies of binding for the CBM2b-1-CBM2b-2 construct, CBM2b-1, and CBM2b-2. From the data in Table 1, this is approximately 4.3 kcal mol^{-1}. An alternative representation would be to express this as a dimensionless constant, described as *Coop* by Creighton (*39*), which describes how much greater the effective concentration of the second module is when attached to the first module. It is given by

$$\Delta G^S = -RT \ln(Coop)$$

and has a value of approximately 2600 (as compared to a value of 1 in the absence of synergy). There is therefore a significant degree of synergy in this system.

Synergy between the family 2b CBMs was also observed when binding to ASC. Both individual CBMs showed extremely weak affinity for ASC, which was only really distinguishable from the background nonspecific binding of GST at high protein concentrations. However, when combined into the same polypeptide chain, in full-length Cf Xyn11A and CBM2b-1-CBM2b-2, the modules displayed a significant increase in affinity for the insoluble ligand. The precise mechanism of the weak cellulose binding in the individual family 2b CBMs is presently unclear. It is interesting to note, however, that the full-length enzyme does not interact with BMCC. This result is similar to that observed for the family 4 CBMs from Cf Cel9B, which can also bind to ASC, but not BMCC. ASC is a relatively unstructured form of cellulose which, although poorly characterized, appears to consist of a certain proportion of individual cellulose chains (*9*). In contrast, BMCC is composed mainly of highly ordered crystalline microfibrils in which multiple chains are strongly bonded to one another

(*30*). In CBM4, the binding site is a cleft that can only accommodate a single cellulose chain, and thus can only interact with soluble cellulose or ASC. It is apparent from the above discussion that the binding specificity of the family 2b CBMs from Cf Xyn11A suggests that these modules may also interact with a single cellulose chain. This view is supported by data presented in this and a previous report (*20*) that shows that both CBM2bs can bind to cellohexaose, albeit weakly, with an estimated K_a of $<1.0 \times 10^2$. The actual binding site for cellohexaose (and by implication cellulose) on the family 2b CBMs appears to be the same as that for xylohexaose, as NMR data show that the same residues are perturbed on the addition of either oligosaccharide. However, in the binding site of family 2b CBMs, the two tryptophans are orientated at approximately 90° to one another on the surface of the protein to allow face-to-face stacking between the aromatic residues and the sugar rings of the 3-fold helical xylan chain. It is difficult to envisage, therefore, a planar molecule such as crystalline cellulose interacting with both perpendicular tryptophans. However, as cellohexaose is more flexible than crystalline cellulose, it is possible that it adopts a more twisted structure in the CBM2b cleft and is thus able to form weak stacking interactions with the two aromatic residues. Similarly, it is possible that some of the cellulose chains in the amorphous regions of ASC are also in a nonplanar orientation and are able to stack, albeit poorly, with the exposed tryptophans in the CBM2bs. Alternatively, one could argue that the synergy for ASC between CBM2b-1 and CBM2b-2 is due to the capacity of the planar tryptophan in each of the CBM2bs to bind to the flat surface of ASC. This is unlikely, however, as removal of the perpendicular tryptophan in CBM2b-1, through the W259A mutation, virtually abolishes cellulose binding in the full-length protein. Furthermore, the loss of cellulose binding which is also seen with the W291A mutation suggests that both exposed tryptophans are involved in the interaction with the glucose polymer.

The ITC data indicate that the interaction of the CBM2b-2 with soluble xylan is enthalpically driven, with an unfavorable entropic contribution; the loss of entropy during the binding event, caused by conformational restriction of the polysaccharide, is greater than the increase in entropy through the release of water molecules from the surface of the protein and carbohydrate. These thermodynamic parameters are similar to those observed with CBM2b-1 and other CBMs that bind soluble polysaccharides (*5*, *9*, *23*).

Although the data presented in this paper, coupled with the work of Linder et al. (*21*), suggest that glycoside hydrolases which contain multiple CBMs exhibit increased affinity for insoluble polysaccharides through the cooperative interactions of these modules, reports on other multiple CBMs do not support this view. Thus, the two family 4 CBMs of Cf Cel9B and the CBM4s from Rm. Xyn10A contribute independently to the individual enzyme's affinity for ASC (*9*, *23*, *24*). Similarly, no synergy is apparent between the CBM2a and CBM10 of Pc Xyn10A binding to insoluble forms of cellulose (*4*). The lack of synergy between the family 4 CBMs appears to reflect their respective orientation with each other, which is fixed as there is no flexible linker between these modules. NMR studies suggest that the binding clefts of the Cf Cel9B CBM4s are positioned side-by-side and not end-to-end (*23*). Thus, the modules cannot bind simultaneously to adjacent sites on the same cellulose chain. It has been suggested that the function of the CBM4s in Cel9B is to sequester cellooligosaccharides away from crystalline cellulose, preventing them from reassociating with the insoluble polysaccharide (*9*). If this scenario is correct, then the reiteration of CBM4s in the enzyme would increase the amount of oligosaccharide that could be sequestered away from the crystalline surface, and this could be the driving force for the presence of two CBM4s in this and other similar enzymes. Although the lack of a flexible linker between the family 4 CBMs explains the absence of synergy seen in Cf Cel9B and Rm Xyn10A, it does not offer an explanation for the noncooperative binding observed between the linked CBMs in Pc Xyn10A. However, the CBMs in this enzyme are from different families and exhibit significantly different affinities for insoluble cellulose, with CBM2a having a 7-fold higher affinity for the insoluble polysaccharide than CBM10. The affinity of the full-length enzyme is similar to CBM2a alone, suggesting that, in this instance, the higher affinity CBM is dominating ligand binding (*4*).

Although the synergy between the CBM2bs in Cf Xyn11A is not reflected in Pc Xyn10A and Cf Cel9B, it is likely that other enzymes with multiple CBMs from the same family that are joined by flexible linkers will have a high affinity for polysaccharides through the cooperative interactions of these modules. Numerous glycoside hydrolases conform to these parameters, and we propose, based on this study and the work of Linder et al. (*21*), that synergy in ligand binding will be evident between the CBMs in these enzymes.

Cf Xyn11A has a 17-fold higher affinity for insoluble xylan than for cellulose. The biological significance of these different affinities is a matter of debate. It could be argued that the capacity of the enzyme to interact with both cellulose and xylan increases the frequency with which the xylanase associates with the plant cell wall, leading to enhanced catalysis. Indeed, many hemicellulases contain specific cellulose-binding modules, which, in some cases, have been shown to increase enzyme activity against cellulose/hemicellulose composites (*2*, *40*, *41*). However, the relative abundance of specific cellulose binding modules in microbial plant cell wall degrading enzyme systems, and the ease with which these enzymes appear to acquire new modules, either from duplication of the microbe's own genome, or via horizontal gene transfer, suggests that if the capacity to bind to cellulose enhanced Xyn11A activity significantly, the enzyme would contain a specific cellulose-binding module. Therefore, it is more likely that the multiple CBM2bs in Cf Xyn11A have evolved to enable the enzyme to bind more tightly to xylan, and that their relatively weak cellulose binding is simply a bystander effect.

In conclusion, this paper demonstrates that the structure and ligand specificity of the two CBM2bs in Cf Xyn11A are essentially identical. The binding properties of full-length and truncated forms of the xylanase demonstrate, for the first time, that discrete CBMs in a modular glycoside hydrolase can act in synergy to bind xylan and cellulose. We propose, therefore, that the evolutionary rationale for the presence of multiple CBMs in glycoside hydrolases, which are from the same family and joined by flexible linker sequences, is to facilitate more efficient binding of these enzymes to polysaccharides within the plant cell wall. Although the rationale

for the presence of multiple CBMs in some glycoside hydrolases would appear to be different, comparison of sequences suggests that synergistic binding may be a common phenomenon.

REFERENCES

1. Tomme, P., Warren, R. A. J., and Gilkes, N. R. (1995) *Adv. Microb. Physiol. 37*, 1−81.
2. Black, G. W., Rixon, J. E., Clarke, J. H., Hazlewood, G. P., Theodorou, M. K., Morris, P., and Gilbert, H. J. (1996) *Biochem. J. 319*, 515−520.
3. Bolam, D. N., Ciruela, A., McQueen-Mason, S., Simpson, P., and Williamson, M. P. (1998) *Biochem. J. 331*, 775−781.
4. Gill, J., Rixon, J. E., Bolam, D. N., McQueen-Mason, S. J., Simpson, P., Williamson, M. P., Hazlewood, G. P., and Gilbert, H. J. (1999) *Biochem. J. 342*, 473−480.
5. Charnock, S. J., Bolam, D. N., Turkenburg, J. P., Gilbert, H. J., Ferreira, L. M. A., Davies, G. J., Fontes, C. M. G. A. (2000) *Biochemistry 39*, 5013−5021.
6. Sun, J. L., Sakka, K., Karita, S., Kimura, T., and Ohmiya, K. (1998) *J. Ferment. Bioeng. 85*, 63−68.
7. Din, N., Damude, H. G., Gilkes, N. R., Miller, R. C., Warren, R. A. J., and Kilburn, D. G. (1994) *Proc. Natl. Acad. Sci. U.S.A. 91*, 11383−11387.
8. Din, N., Gilkes, N. R., Tekant, B., Miller, R. C., Warren, R. A. J., and Kilburn, D. G. (1991) *Bio/Technol. 9*, 1096−1099.
9. Tomme, P., Creagh, A. L., Kilburn, D. G., and Haynes, C. A. (1996) *Biochemistry 35*, 13885−13894.
10. Sakon, J., Irwin, D., Wilson, D. B., and Karplus, P. A. (1997) *Nat. Struct. Biol. 4*, 810−817.
11. Irwin, D., Shin, D.-H., Zhang, S., Barr, B. K., Sakon, J., Karplus, P. A., and Wilson, D. B. (1998) *J. Bacteriol. 180*, 1709−1714.
12. Southall, S. M., Simpson, P. J., Gilbert, H. J., Williamson, G., and Williamson M. P. (1999) *FEBS Lett. 447*, 58−60.
13. Coutinho, P. M., and Henrissat, B. (1999) in *Recent Advances in Carbohydrate Bioengineering* (Gilbert, H. J., Davies, G. J., Henrissat, B., and Svensson, B., Eds.) pp 3−12, The Royal Society of Chemistry, Cambridge.
14. Kraulis, P. J., Clore, G. M., Nilges, M., Jones, T. A., Peterson, G., Knowles, J., and Gronenborn, A. M. (1989) *Biochemistry 28*, 7241−757.
15. Xu, G. Y., Ong, E., Gilkes, N. R., Kilburn, D. G., Muhindaram, D. R., Harris-Brandts, M., Carver, J. P., Kay, L. E., and Harvey, T. S. (1995) *Biochemistry 34*, 6993−7009.
16. Tormo, J., Lamed, R., Chirino, A. J., Morag, E., Bayer, E. A., Shoham, Y., and Steitz, T. A. (1996) *EMBO J. 15*, 5739−5751.
17. Brun, E., Moriaud, F., Gans, P., Blackledge, M. J., Barras, F., and Marion, D. (1997) *Biochemistry 36*, 16074−16086.
18. Raghothama, S., Simpson, P. J., Szabó, L., Nagy, T., Gilbert, H. J., and Williamson, M. P. (2000) *Biochemistry 39*, 978−984.
19. Johnson, P. E., Joshi, M. D., Tomme, P., Kilburn, D. G., and McIntosh, L. P. (1996) *Biochemistry 35*, 14381−14394.
20. Simpson, P. J., Bolam, D. N., Cooper, A., Ciruela, A., Hazlewood, G. P., Gilbert, H. J., and Williamson, M. P. (1999) *Structure 7*, 853−864.
21. Linder, M., Salovouri, I., Ruohonen, L., and Teeri, T. T. (1996) *J. Biol. Chem. 271*, 21268−21272.
22. Boraston, A. B., Tomme, P., Amandoron, E. A., and Kilburn, D. G. (2000) *Biochem. J. 350*, 933−941.
23. Brun, E., Johnson, P. E., Creagh, A. L., Tomme, P., Webster, P., Haynes, C. A., and McIntosh, L. P. (2000) *Biochemistry 39*, 2445−2458.
24. Abou Hachem, M., Nordberg Karlsson, E., Bartonek-Roxå, E., Raghothama, S., Simpson, P. J., Gilbert, H. J., Williamson, M. P., and Holst, O. (2000) *Biochem. J. 345*, 53−60.
25. Laurie, J. I., Clarke, J. H., Ciruela, A., Faulds, C. D., Williamson, G., Gilbert, H. J., Rixon, J. E., Millward-Sadler, J., and Hazlewood, G. P. (1997) *FEMS Microbiol. Lett. 148*, 261−264.
26. Clark, J. H., Laurie, J. I., Gilbert, H. J., and Hazlewood, G. P. (1991) *FEMS Microbiol. Lett. 83*, 305−310.
27. Millward-Sadler, S. J., Poole, D. M., Henrissat, B., Hazlewood, G. P., Clarke, J. H., and Gilbert, H. J. (1994) *Mol. Microbiol. 11*, 375−382.
28. Black, G. W., Hazlewood, G. P., Millward-Sadler, S. J., Laurie, J. I., and Gilbert, H. G. (1995) *Biochem. J. 307*, 191−195.
29. Simpson, P. J., Hefang, X., Bolam, D. N., Gilbert, H. J., Williamson, M. P. (2000) *J. Biol. Chem. 275*, 41137−41142.
30. Gilkes, N. R., Jervis, E., Henrissat, B., Tekant, B., Miller, R. C. Jr., Warren, R. A. J., and Kilburn, D. G. (1992) *J. Biol. Chem. 267*, 6743−6749.
31. Ghangas, G. S., Hu, Y.-J., and Wilson, D. B. (1989) *J. Bacteriol. 171*, 2963−2969.
32. Norrander, J., Kempe, T., and Messing, J. (1983) *Gene 26*, 101−106.
33. Studier, F. W., and Moffat, B. A. (1986) *J. Mol. Biol. 189*, 113−130.
34. Baxter, N. J., and Williamson, M. P. (1997) *J. Biomol. NMR 9*, 359−369.
35. Nilges, M. (1995) *J. Mol. Biol. 245*, 645−660.
36. Laskowski, R. A., Rullmann, J. A. C., MacArthur, M. W., Kaptein, R., and Thornton, J. M., (1996) *J. Biomol. NMR 8*, 477−486.
37. Weis, W. I., and Drickamer, K. (1996) *Annu. Rev. Biochem. 65*, 441−473.
38. Lis, H., and Sharon, N. (1998) *Chem. Rev. 98*, 637−674.40.
39. Creighton, T. E. (1996) in *Proteins Structures and Molecular Properties*, 2nd Ed., p 166, W. H. Freeman and Co., New York.
40. Kellet, L. E., Poole, D. M., Ferreira, L. M. A., Durrant, A. J., Hazlewood, G. P., and Gilbert, H. J. (1990) *Biochem. J. 272*, 369−376.
41. Ferreira, L. M. A., Wood, T. M., Williamson, G., Faulds, C., Hazlewood, G. P., Black, G. W., and Gilbert, H. J. (1993) *Biochem. J. 294*, 349−355.
42. Kraulis, P. (1991) *J. Appl. Crystallogr. 24*, 946−950.

BI002564L